

2-12-2011

# Micro-CT Characterization of Human Trabecular Bone in Osteogenesis Imperfecta

John Jameson

*Marquette University, john.jameson@marquette.edu*

Carolyne Albert

*Marquette University, carolyne.albert@marquette.edu*

Peter Smith

*Orthopaedic & Rehabilitation Engineering Center*

Robert C. Molthen

*Marquette University, robert.molthen@marquette.edu*

Gerald F. Harris

*Marquette University, gerald.harris@marquette.edu*

---

Published version. Published as part of the proceedings of the conference, *SPIE 7965, Medical Imaging 2011: Biomedical Applications in Molecular, Structural, and Functional Imaging*, 2011. DOI. © 2011 Society of Photo-optical Instrumentation Engineers (SPIE). Used with permission.

# Micro-CT characterization of human trabecular bone in osteogenesis imperfecta

John Jameson<sup>1,2</sup>, Carlyne Albert<sup>1,2</sup>, Peter Smith<sup>2,3</sup>, Robert Molthen<sup>1,2,4,5</sup> & Gerald Harris<sup>1,2,3</sup>

<sup>1</sup>Department of Biomedical Engineering, Marquette University, Milwaukee, WI, USA

<sup>2</sup>Orthopaedic & Rehabilitation Engineering Center, Milwaukee, WI, USA

<sup>3</sup>Shriners Hospitals for Children, Chicago, IL, USA

<sup>4</sup>Department of Medicine, Medical College of Wisconsin, Milwaukee, WI, USA

<sup>5</sup>Department of Veterans Affairs, Zablocki VA Medical Center, Milwaukee, WI, USA

## ABSTRACT

Osteogenesis imperfecta (OI) is a genetic syndrome affecting collagen synthesis and assembly. Its symptoms vary widely but commonly include bone fragility, reduced stature, and bone deformity. Because of the small size and paucity of human specimens, there is a lack of biomechanical data for OI bone. Most literature has focused on histomorphometric analyses, which rely on assumptions to extrapolate 3-D properties. In this study, a micro-computed tomography ( $\mu$ CT) system was used to directly measure structural and mineral properties in pediatric OI bone collected during routine surgical procedures. Surface renderings suggested a poorly organized, plate-like orientation. Patients with a history of bone-augmenting drugs exhibited increased bone volume fraction (BV/TV), trabecular number (Tb.N), and connectivity density (Eu.Conn.D). The latter two parameters appeared to be related to OI severity. Structural results were consistently higher than those reported in a previous histomorphometric study, but these differences can be attributed to factors such as specimen collection site, drug therapy, and assumptions associated with histomorphometry. Mineral testing revealed strong correlations with several structural parameters, highlighting the importance of a dual approach in trabecular bone testing. This study reports some of the first quantitative  $\mu$ CT data of human OI bone, and it suggests compelling possibilities for the future of OI bone assessment.

**Keywords:** Osteogenesis imperfecta,  $\mu$ CT, bone histomorphometry, trabecular bone, trabecular structure, bone mineral density, connectivity

---

Further author information: (Send correspondence to J.J.)  
J.J.: E-mail: john.jameson@marquette.edu, Telephone: +1-414-288-8497

Medical Imaging 2011: Biomedical Applications in Molecular, Structural, and Functional Imaging,  
edited by John B. Weaver, Robert C. Molthen, Proc. of SPIE Vol. 7965, 79650I · ©  
2011 SPIE · CCC code: 0277-786X/11/\$18 · doi: 10.1117/12.877586

## 1. INTRODUCTION

Osteogenesis imperfecta (OI) is a heritable bone fragility syndrome affecting between 20,000 and 50,000 people in the United States.<sup>1</sup> It is commonly characterized by mutations in the genes that code for type I collagen or its associated proteins. Bone tissue is formed by mineral deposition onto this collagen scaffolding, so it is not surprising that deficiencies in the framework have negative implications on bone performance. Since type I collagen is one of the most ubiquitous structural proteins in the body, OI commonly affects other tissues such as lung and ligaments, as well as sensory machinery associated with the auditory and visual systems. This leads to a myriad of symptoms including bone fragility and deformity, decreased stature, tinted sclerae, hearing loss, and respiratory problems.<sup>2</sup> Patients are currently classified into one of eight known clinical types of OI, with each group sharing common genetic mutations and symptoms.<sup>1</sup>

Since OI is a genetic disorder, and gene therapies currently lack viability, most treatments have focused on improving mobility and quality of life.<sup>2</sup> However, additional clinical tools would be useful for diagnosis and assessment of fracture risk. Similar to other engineering materials, the functional strength of bone depends not only on its properties but also its structure. To date most bone studies have focused primarily on bone mineral density (BMD) as the main determinant of strength, leaving structural information such as material distribution and trabecular architecture largely unaddressed. Both mineral and structural parameters are typically determined using 2-D techniques such as dual-energy X-ray absorptiometry (DEXA) and histology. Although these methods have become widely accepted by clinical standards,<sup>2</sup> they suffer several deficiencies. By nature, *in vivo* DEXA scans subject patients to ionizing radiation, which poses a continuing concern for OI patients, who routinely undergo multiple annual X-ray scans (e.g. for fractures, deformity mapping, follow-ups, etc.). DEXA also integrates mineral information in 2-D space and only provides mean values across samples, so 3-D depth information that may be fundamentally important is lost. Because of these (and other) shortcomings, some researchers question the ability of DEXA alone to predict fracture, especially in the growing skeleton.<sup>3</sup> Furthermore, histology requires destructive tissue processing and relies on geometric and material distribution assumptions to extrapolate 3-D properties from 2-D slides.

Alternatively, micro-computed tomography ( $\mu$ CT) allows for the 3-D analysis of BMD and bone microstructure.<sup>4</sup> This modality is especially useful for OI research because patients routinely undergo corrective surgeries that involve removal of small bone fragments, which would normally be discarded post-operatively. The purpose of this study was to investigate  $\mu$ CT as a method to characterize properties of OI bone in several of these fragments, and to compare the results to previous OI studies. Correlations were also performed to determine possible relationships among the different parameters.

## 2. MATERIALS AND METHODS

### 2.1. $\mu$ CT imaging

A total of 8 fragments were collected from lower extremity long bones (femur or tibia) in 5 patients (sex: 2M, 3F; age range: 1.5-11.5 years) under written informed consent/assent and institutional IRB approval during routine osteotomy surgical procedures (Shriners Hospitals for Children, Chicago, IL). All patients were diagnosed with moderate to severe OI (types IV or III, respectively), and 3 of the 5 patients had received at least one round of a bisphosphonate to increase bone mass. The bone fragments were scanned using a customized  $\mu$ CT system developed at the Zablocki VA Medical Center (RM, Milwaukee, WI). A detailed description of the system has been provided elsewhere.<sup>5</sup> Briefly, the hardware consists of a microfocal X-ray source (3- $\mu$ m focal spot; Comet North America), an AI-5830-HP image intensifier (North American Imaging) coupled to a Silicon Mountain Design SMD1M-15 CCD camera (DALSA), and a specimen micro-manipulator stage, all mounted on a precision rail. Specimens were thawed and scanned in continuous mode (33 kVp, 231  $\mu$ A, 360 views, 7-frame average) in saline at 35- $\mu$ m isotropic voxel resolution. Prior to reconstruction, a ring artifact reduction algorithm was performed on the preprocessed projection images. After reconstruction with a Feldkamp cone beam algorithm, attenuation intensity values were converted to Hounsfield units (HU) by applying the following scaling algorithm:

$$HU(x, y, z) = 1000 \frac{CT(x, y, z) - CT_w}{CT_w - CT_a}, \quad (1)$$

where  $CT(x, y, z)$ ,  $CT_w$ , and  $CT_a$  correspond to the reconstructed intensity values of the image, water (taken from a separate scan), and air, respectively.

## 2.2. Bone morphometry

Trabecular volumes of interest (VOIs) were identified from the resulting floating point image volumes and analyzed for several structural parameters in MicroView (v2.1.2; GE Healthcare). Cubic VOIs (2-mm side length) were segmented by applying a local threshold determined using the Auto-Threshold option in MicroView, which utilizes an Otsu cluster thresholding algorithm to minimize the weighted sum of within-class variances of foreground (bone) and background (non-bone) pixels.<sup>6</sup> This feature has been used previously for segmentation of bone in  $\mu$ CT data.<sup>7</sup> Each VOI was examined using the Bone Analysis tool, which directly measures bone volume fraction (BV/TV) and bone surface fraction (BS/BV). From these quantities, the algorithm then uses the following parallel plate model equations<sup>8</sup> to calculate several other standard morphometric parameters, including trabecular thickness (Tb.Th), number (Tb.N), and separation (Tb.Sp):

$$Tb.Th = \frac{2}{BS/BV} \quad (2)$$

$$Tb.N = \frac{BV/TV}{Tb.Th} \quad (3)$$

$$Tb.Sp = \frac{1}{Tb.N} - Tb.Th. \quad (4)$$

Connectivity was determined by calculating the Euler number ( $\chi$ ) of the 3-D trabecular network ( $X$ ):

$$\chi(X) = \beta_0 - \beta_1 + \beta_2, \quad (5)$$

where  $\beta_0$  is the number of bone objects,  $\beta_1$  is the connectivity, and  $\beta_2$  is the number of enclosed marrow cavities. After performing a purification step, the trabecular region is assumed to be a single connected structure ( $\beta_0=1$ ) with no isolated marrow cavities ( $\beta_2=0$ ).<sup>9</sup> Thus highly connected tissues (such as healthy trabecular bone) have large, negative Euler numbers.<sup>10</sup> Connectivity density (Eu.Conn.D), which measures the number of redundant connections between trabecular structures per unit volume, was then calculated by solving for  $\beta_1$  in equation (5) and dividing it by the volume of the VOI. After the specimens were analyzed, 3-D surface-shaded renderings were produced for visualization using the Isosurface Tool.

## 2.3. BMD

Volumetric BMD, tissue mineral density (TMD), and bone mineral content (BMC), were calculated for the trabecular VOIs using a phantom (Image Analysis, Inc., Columbia, KY) having three different hydroxyapatite (HA) concentrations (0, 75, and 150 mg HA/cm<sup>3</sup>). A linear curve relating  $\mu$ CT numbers (in HU) and HA concentration (in mg HA/cm<sup>3</sup>) was then generated and used to determine the input value for bone in MicroView's Bone Analysis tool. The lower bound on intensity values was set to exclude the background.

# 3. RESULTS

## 3.1. $\mu$ CT data

Examination of the reconstructed cubic VOIs showed a general plate-like structure, which is common for lower extremity long bones (Figure 1). Unlike healthy bone, the OI trabecular plates did not seem to follow any preferential orientation, suggesting a less organized architecture. Surprisingly, the specimens from one of the severe (type III) OI patients seemed to best follow the parallel plate bone model (Figure 1, G-H). However, the effects of factors such as drug treatment, harvest site, gender, and OI (genetic) type were not obviously distinguishable.



### 3.2. Bone morphometry

Results from the structural analysis are summarized in Table 1. All parameters were moderately heterogeneous across the sample population. Both Tb.N and Eu.Conn.D showed a general indirect relationship with severity of OI, where type III patients seemed to have less trabeculae and lower connectivity than those with either type IV or III/IV. Several indices including BV/TV, Tb.N, and Eu.Conn.D were elevated in patients who had received at least one round of a bisphosphonate prior to specimen harvesting. One patient who received such treatments between the first (4-A) and second (4-B) specimen collections exhibited modest increases in BV/TV and Tb.Th, but decreases in the other parameters.

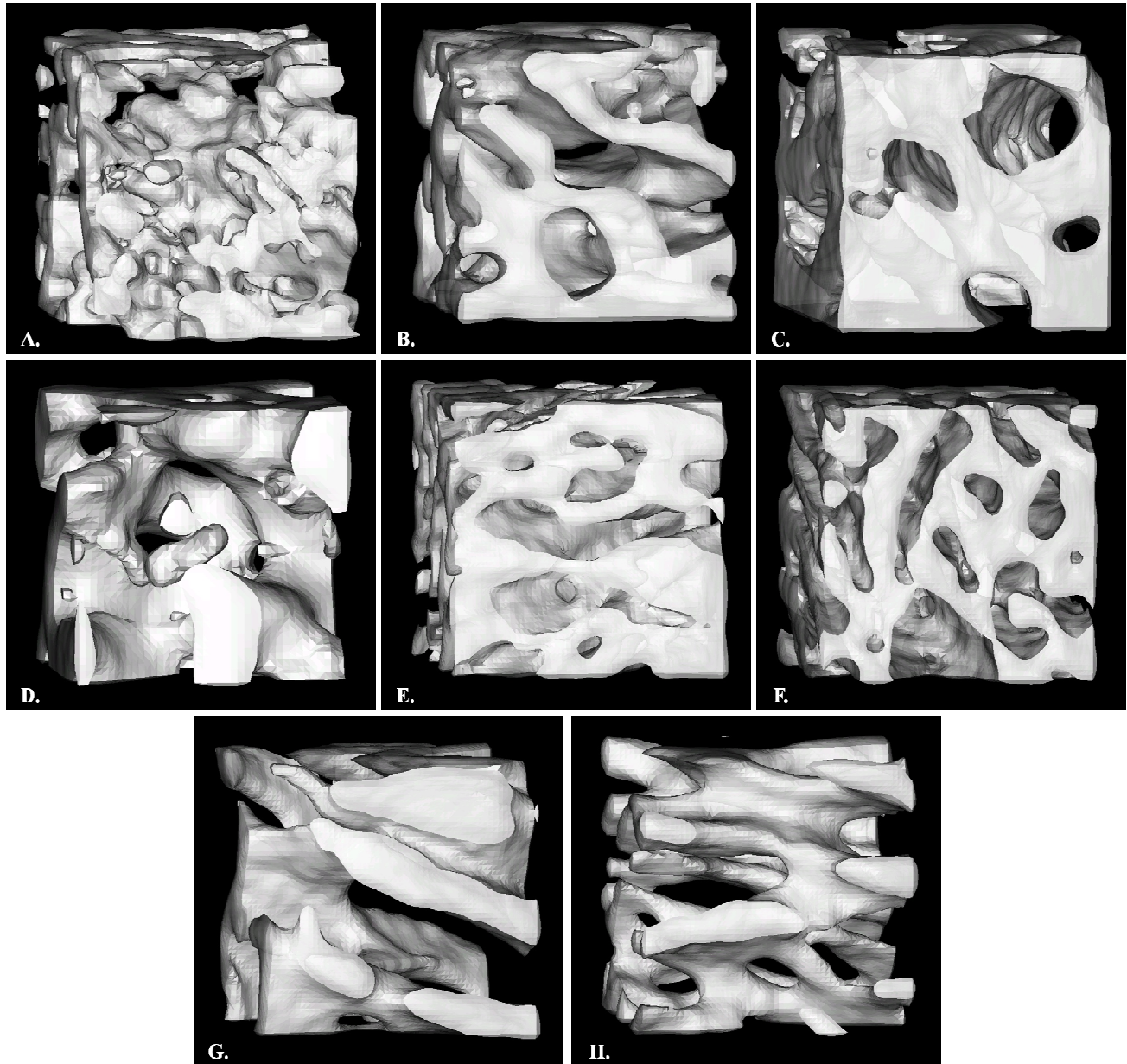


Figure 1: Surface-shaded renderings of trabecular VOIs. A-B: Patient 1; C: Patient 2; D: Patient 3; E-F: Patient 4; G-H: Patient 5.

Table 1: Bone morphometric parameters.

<i>Specimen</i>	<i>OI Type</i>	<i>BV/TV</i>	<i>BS/BV</i> (1/mm)	<i>Tb.Th</i> (mm)	<i>Tb.N</i> (1/mm)	<i>Tb.Sp</i> (mm)	<i>Eu.Conn.D</i> (1/mm <sup>3</sup> )
1-A*	IV	0.41	13.54	0.15	2.77	0.21	21.74
1-B*	IV	0.48	9.00	0.22	2.18	0.24	7.98
2	III	0.64	5.60	0.36	1.78	0.20	4.86
3*	III	0.43	8.34	0.24	1.79	0.32	7.13
4-A*	III/IV	0.41	14.52	0.14	2.98	0.20	18.02
4-B*	III/IV	0.58	9.35	0.21	2.73	0.15	10.78
5-A	III	0.28	9.37	0.21	1.33	0.54	1.84
5-B	III	0.26	13.19	0.15	1.74	0.42	3.84
<b>Median (Range):</b>		<b>0.42 (0.37)</b>	<b>9.36 (8.92)</b>	<b>0.21 (0.22)</b>	<b>1.99 (1.65)</b>	<b>0.23 (0.38)</b>	<b>7.56 (19.9)</b>

\*Patient received bisphosphonate treatment prior to specimen harvesting.

### 3.3. BMD

Results from the BMD tests are summarized in Table 2. This analysis did not reveal any clear relationships between OI severity and bone mineral metrics. However, patients who received drug therapy showed trends of increased BMD and BMC compared to untreated peers. Similar to the structural results, the patient who underwent drug treatment between specimen collections exhibited substantial increases in all mineral parameters (Table 2, specimens 4-A and 4-B).

Table 2: BMD calculations.

<i>Specimen</i>	<i>OI Type</i>	<i>BMD (mg/cm<sup>3</sup>)</i>	<i>TMD (mg/cm<sup>3</sup>)</i>	<i>BMC (mg)</i>
1-A*	IV	232.3	564.6	1.87
1-B*	IV	411.6	831.2	3.25
2	III	558.1	868.3	4.48
3*	III	400.0	907.3	1.36
4-A*	III/IV	278.6	661.9	2.24
4-B*	III/IV	470.6	806.8	3.78
5-A	III	228.9	791.4	1.84
5-B	III	200.8	759.2	1.61
<b>Median (Range):</b>		<b>339.3 (357.2)</b>	<b>799.1 (342.7)</b>	<b>2.05 (3.13)</b>

\*Patient received bisphosphonate treatment prior to specimen harvesting.

## 4. DISCUSSION

In this study,  $\mu$ CT was used to analyze several quantitative measures of trabecular microstructure and mineralization in pediatric bone specimens from children with moderate to severe OI. To date there is surprisingly little data examining how OI affects bone development. Several historic studies have used standard histomorphometric procedures to examine small OI populations.<sup>11-13</sup> However, none of these were able to offer conclusive results, as one<sup>12</sup> only studied adults and the others tested very small clinical populations ( $n < 10$ ). The most extensive study to date used histomorphometric methods on 70 OI patients and 27 age-matched controls, finding significant decreases in BV/TV, Tb.N, and Tb.Th for OI patients.<sup>14</sup> Minimal differences in trabecular parameters were reported between types III and IV OI. Of particular note was that pharmacological therapy was an exclusion criterion.

The structural metrics reported in the current study were generally higher than those reported in the aforementioned OI histomorphometric studies. There are, however, many explanations for the apparent discrepancies. Traditional histological methods test bone biopsies from the iliac crest, while all of the specimens in the current study were collected

from lower extremity long bones. Additionally, histology relies on assumptions to extract 3-D bone parameters from 2-D slides, which can lead to more conservative values. Most of our specimens also came from patients who had received drugs to enhance bone mass. It is widely accepted that these drugs affect both mineral and structural indices, and we were able to observe these effects despite a small sample size.

One interesting observation from our study was that connectivity density and Tb.N were highly correlated ( $R^2=0.81$ ) and seemed related to severity of OI. This could be an important diagnostic tool for distinguishing OI type in patients who present heterogeneous symptoms. For example, one of the patients from our study was diagnosed with type III/IV OI based on clinical observations. Comparison to the other specimens scanned for this study suggests that this patient's indices are more similar to the other type IV patients.

Simple linear regression analyses suggest strong correlations between the morphometric and mineral parameters (Figure 2). The strongest structural correlations with BMD, TMD, and BMC were BV/TV, BS/BV, and BV/TV, respectively. The fact that BV/TV was strongly related to two of these mineral parameters underscores the importance of considering both structure and bone mass when analyzing trabecular bone.

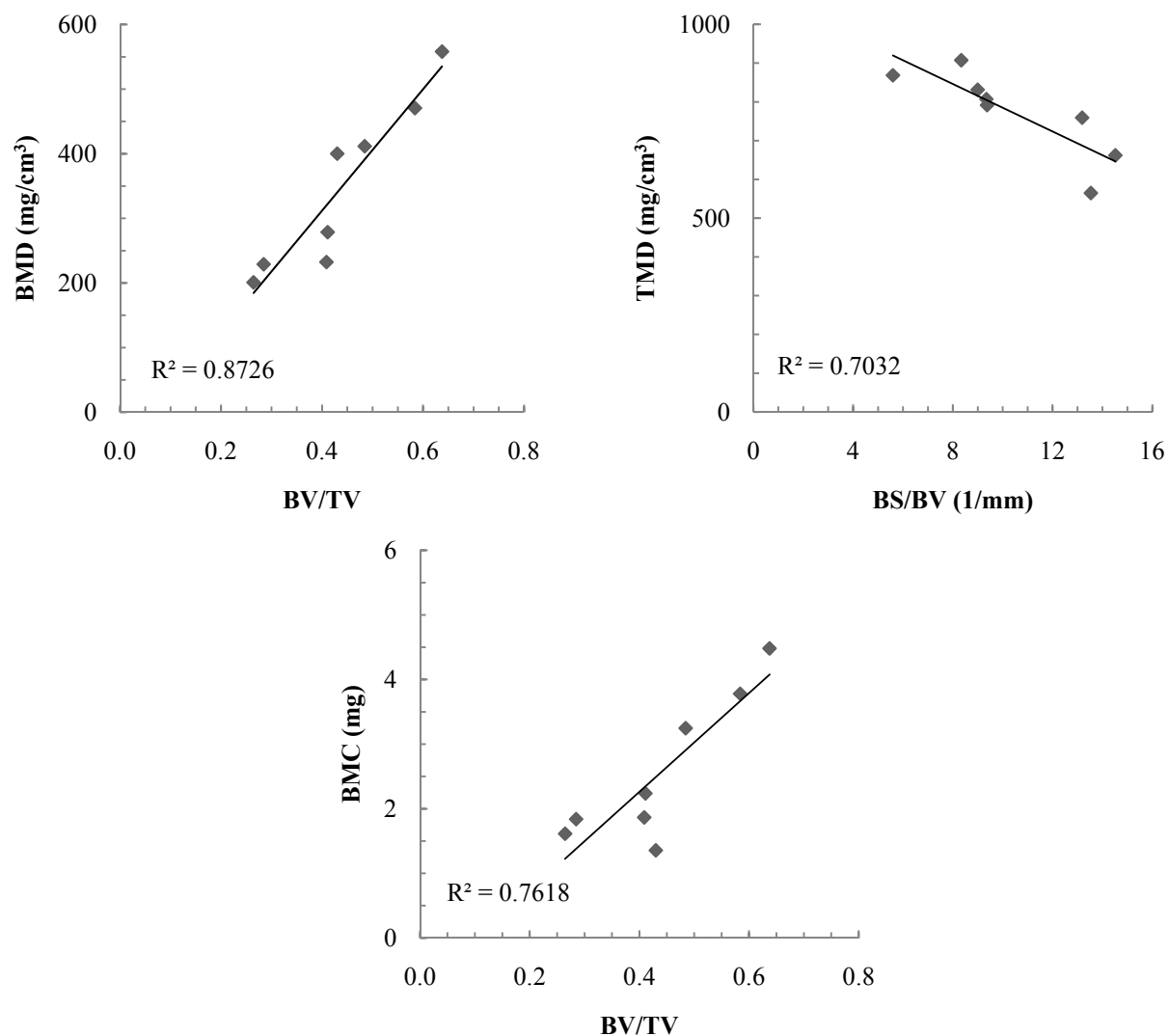


Figure 2: Correlations between architectural and mineral parameters.

Because our methods are still under development, we present our data as a preliminary assessment of the possibilities of  $\mu$ CT for OI bone testing. We acknowledge several potential confounding factors associated with this study. The fragments collected for testing came from multiple bones (femora and tibia), and the exact anatomical locations within the bones were not rigorously recorded. Most specimens came from patients with a history of anti-resorptive drugs.

## 5. CONCLUSIONS

In this study,  $\mu$ CT was used as an alternative to standard histological methods for the calculation of 3-D properties of human trabecular bone in OI. Unlike histology, our methods do not require chemical processing, nor do they rely on geometric or material assumptions to extrapolate 3-D parameters from 2-D sections. Similarly, our BMD calculations on excised specimens eliminate concerns with radiation dose associated with the current clinical practice (i.e. DEXA scans). Our results suggest relationships between OI severity and structural parameters such as Tb.N and connectivity density. Furthermore, we report strong correlations among structural and mineral metrics. While values of our morphometric parameters are generally higher than reported in previous OI studies, these differences can be accounted for by alterations in study design and such factors as collection site locus, assessment technique, and drug treatment. In addition to presenting some of the first quantitative  $\mu$ CT data on human OI bone, this study provides compelling evidence for the continued use of  $\mu$ CT in OI bone analysis.

## ACKNOWLEDGEMENTS

This work was supported by OREC, the Dr. Ralph and Marian Falk Medical Research Trust, NIDRR Grants H133G050201 and H133E100007, and the Department of Veterans Affairs.

## REFERENCES

- [1] <http://www.oif.org/site/PageServer>
- [2] Chiasson R.M., Munns C., and Zeitlin L. (eds.), [Interdisciplinary treatment approach for children with osteogenesis imperfecta], Shriners Press, 1-87 (2004).
- [3] Petit M.A., Beck T.J., and Kontulainen S.A., "Examining the developing bone: What do we measure and how do we do it?" *J Musculoskelet Neuronal Interact* 5 (3), 213-224 (2005).
- [4] Kalpakcioglu B.B., Morshed S., Engelke K., and Genant H.K., "Advanced imaging of bone macrostructure and microstructure in bone fragility and fracture repair," *J Bone Joint Surg Am* 90, 68-78 (2008).
- [5] Karau K.L., Johnson R.H., Molthen R.C., Dhyani A.H., Haworth S.T., Hanger C.C., Roerig D.L., and Dawson C.A., "Microfocal X-ray CT imaging and pulmonary arterial distensibility in excised rat lungs," *Am J Physiol* 281, H1447-H1457 (2001).
- [6] Sezgin M. and Sankur B., "Survey over image thresholding techniques and quantitative performance evaluation," *Journal of Electronic Imaging* 13, 146-165 (2004).
- [7] Ling Y., Rios H.F., Myers E.R., Lu Y., Feng J.Q., and Boskey A.L., "DMP1 Depletion decreases bone mineralization in vivo: An FTIR imaging analysis," *JBMR* 20, 2169-2177 (2005).
- [8] Parfitt A.M., Mathews C.H.E., Villanueva A.R., Kleerekoper M., Frame B., and Rao D.S., "Relationship between surface, volume, and thickness of the iliac trabecular bone in aging and in osteoporosis: Implications for the microanatomic and cellular mechanism of bone loss," *J Clin Invest* 72, 1396-1409 (1983).
- [9] Odgaard A. and Gundersen H.J., "Quantification of connectivity in cancellous bone, with special emphasis on 3-D reconstructions," *Bone* 14 (2), 173-182 (1993).

- [10]Feldkamp L.A., Goldstein S.A., Parfitt A.M., Jesion G., and Kleerekoper M., "The direct examination of three-dimensional bone architecture in vitro by computed tomography," *JBMR* 4 (1), 3-11 (1989).
- [11]Baron R.E., Gertner J.M., Lang R., and Vignery A., "Increased bone turnover with decreased bone formation by osteoblasts in children with osteogenesis imperfecta tarda," *Pediatr Res* 17, 204-207 (1983).
- [12]McCarthy E.F., Earnest K., Rossiter K., and Shapiro J., "Bone histomorphometry in adults with type IA osteogenesis imperfecta," *Clin Orthop* 336, 254-262 (1997).
- [13]Ste-Marie L.G., Charhon S.A., Edouard C., Chapuy M.C., and Meunier P.J., "Iliac bone histomorphometry in adults and children with osteogenesis imperfecta," *J Clin Pathol* 37, 1081-1089 (1984).
- [14]Rauch F., Travers R., Parfitt A.M., Glorieux F.H., "Static and dynamic bone histomorphometry in children with osteogenesis imperfecta," *Bone* 26 (6), 581-589 (2000).